Contribution of isovector mesons to the symmetry energy in a microscopic model

Francesca Sammarruca*
Physics Department, University of Idaho, Moscow, Idaho 83844-0903, USA
(Received 22 July 2011; revised manuscript received 6 September 2011; published 10 October 2011)

We examine the potential energy contributions to the symmetry energy (in the parabolic approximation) arising from the isovector mesons, π, ρ, and δ. The significance of a microscopic model that incorporates all important mesons is revealed. In particular, we demonstrate the importance of the pion for a realistic investigation of isospin-sensitive systems.

DOI: 10.1103/PhysRevC.84.044307 PACS number(s): 21.65.Cd, 21.65.Ef, 21.65.Jk, 21.60.−n

I. INTRODUCTION

The physics of unstable nuclei is closely related to the equation of state (EOS) for isospin-asymmetric nuclear matter (IANM). In fact, applications of IANM are broad, ranging from the structure of rare isotopes to the properties of neutron stars. An important quantity that emerges from IANM studies is the so-called symmetry energy. However, in spite of many recent and intense efforts, the density dependence of the symmetry energy is not sufficiently constrained by the available data, and theoretical predictions show considerable model dependence.

Older theoretical studies of IANM can be found in Refs. [1,2]. Interactions adjusted to fit properties of finite nuclei, such as those based on the nonrelativistic Skyrme Hartree-Fock theory [3] or the relativistic mean-field theory (see, for instance, Ref. [4]), have been used to extract phenomenological EOS. A review of Skyrme interactions, particularly popular for nuclear structure applications, can be found in Ref. [5]. Variational calculations of asymmetric matter were reported in Refs. [6,7], whereas extensive microscopic work with IANM was undertaken by Lombardo and collaborators [8,9] within the Brueckner-Hartree-Fock (BHF) approach. Dirac-Brueckner-Hartree-Fock (DBHF) calculations of IANM properties were performed by the Oslo group [10], the Idaho group [11,12], and by Fuchs and collaborators [13].

In this paper, we concentrate on the role of the isovector mesons for the symmetry energy. The latter is defined from an expansion of the energy per nucleon in terms of the isospin asymmetry parameter. In the parabolic approximation, it is simply the difference between the energies per particle in neutron matter and symmetric nuclear matter; see the next section. Physically, it represents the energy "price" a nucleus must pay for being isospin asymmetric.

The isovector mesons and their impact on the symmetry energy have been discussed in the literature, particularly in the context of mean-field approaches, both relativistic and nonrelativistic [see, for instance, Ref. [14] for an extensive review on reaction dynamics with exotic nuclei based on effective interactions derived from quantum hadrodynamics (QHD)]. Recently, considerable interest has developed around the symmetry potential, which arises from the difference between neutron and proton single-particle potentials in isospin-asymmetric matter. With regard to that issue, it is interesting to recall that, in relativistic mean-field approaches, the introduction of the isovector scalar meson (the δ or a_0) is reported to invert the sign of the splitting between the masses of the neutron and the proton in neutron-rich matter [15].

Furthermore, in approaches based on QHD, such as those originally proposed by Walecka and collaborators [16–18], the dynamical degrees of freedom are essentially included through coupling of the nucleons to the isoscalar scalar σ and vector ω mesons. QHD-I models of nuclear matter do not include the pion, which is perhaps the reason why the contribution of the pion to the symmetry energy may have not been discussed in sufficient depth. (Note, however, that Walecka's QHD-II model does include both π and ρ.)

We will explore the role of all isovector channels for the symmetry energy from the point of view of an *ab initio* model. The main point of the *ab initio* approach is that mesons are tightly constrained by the free-space data and their parameters are never readjusted in the medium (this is what we mean by "parameter free"). Furthermore, the contributions from the various mesons are fully iterated, thus giving rise to correlation effects. The corresponding predictions can be dramatically different than those which may be produced in first-order calculations.

This paper is organized as follows: In the next section, we present some facts and phenomenology about the symmetry energy; then, in Sec. III, after a brief review of our theoretical approach, we focus on exploring the potential energy contributions of the isovector mesons to the symmetry energy. Our conclusions are summarized in the last section.

II. SOME FACTS ABOUT IANM

Asymmetric nuclear matter can be characterized by the neutron density ρ_n and the proton density ρ_p, which are related to their respective Fermi momenta, k_F^n and k_F^p, by

$$\rho_i = \frac{\left(k_F^i\right)^3}{3\pi^2}, \tag{1}$$

with $i = n$ or p.

It is more convenient to refer to the total density $\rho = \rho_n + \rho_p$ and the asymmetry (or neutron excess) parameter $\alpha = \frac{\rho_n - \rho_p}{\rho}$. Clearly, $\alpha = 0$ corresponds to symmetric matter,

*fsammarr@uidaho.edu

and $\alpha = 1$ corresponds to neutron matter. In terms of α and the average Fermi momentum k_F, which is related to the total density in the usual way,

$$\rho = \frac{2k_F^3}{3\pi^2}, \tag{2}$$

the neutron and proton Fermi momenta can be expressed as

$$k_F^n = k_F(1+\alpha)^{1/3} \tag{3}$$

and

$$k_F^p = k_F(1-\alpha)^{1/3}, \tag{4}$$

respectively.

Expanding the energy or particle in IANM with respect to the asymmetry parameter yields

$$e(\rho,\alpha) = e_0(\rho) + \frac{1}{2}\left(\frac{\partial^2 e(\rho)}{\partial\alpha^2}\right)_{\alpha=0}\alpha^2 + O(\alpha^4), \tag{5}$$

where the first term is the energy per particle in symmetric matter and the coefficient of the quadratic term is identified with the symmetry energy $e_{\rm sym}$. In the Bethe-Weizsäcker formula for the nuclear binding energy, it represents the amount of binding a nucleus has to lose when the numbers of protons and neutrons are unequal. To a very good degree of approximation, one can write

$$e(\rho,\alpha) \approx e_0(\rho) + e_{\rm sym}(\rho)\alpha^2. \tag{6}$$

The symmetry energy is also closely related to the neutron β decay in dense matter, whose threshold depends on the proton fraction. A typical value for $e_{\rm sym}$ at nuclear-matter density ρ_0 is 30 MeV, with theoretical predictions spreading approximately between 26 and 35 MeV. The effect of a term of fourth order in the asymmetry parameter [$O(\alpha^4)$] on the bulk properties of neutron stars is very small, although it may impact the proton fraction at high density. More generally, nonquadratic terms are usually associated with isovector pairing, which is a surface effect and thus vanishes in infinite matter [19].

Equation (6) displays a convenient separation between the symmetric and asymmetric parts of the EOS, which facilitates the identification of observables that, for instance, may be sensitive mainly to the symmetry energy. Presently, research groups from GSI [20], MSU [21], Italy [22], France [23], and China [24,25] are investigating the density dependence of the symmetry energy through heavy-ion collisions. Based upon recent results, these investigations appear to agree reasonably well on the following parametrization of the symmetry energy:

$$e_{\rm sym}(\rho) = 12.5\,{\rm MeV}\left(\frac{\rho}{\rho_0}\right)^{2/3} + 17.5\,{\rm MeV}\left(\frac{\rho}{\rho_0}\right)^{\gamma_i}, \tag{7}$$

where the first term is the kinetic contribution and γ_i (the exponent appearing in the potential energy part) is found to be between 0.4 and 1.0. Naturally, there are uncertainties associated with all transport models. Recent constraints from MSU [21] were extracted from simulations of ^{112}Sn and ^{124}Sn collisions with an improved quantum molecular dynamics transport model and are consistent with isospin diffusion data and the ratio of neutron and proton spectra.

Typically, parametrizations like the one given in Eq. (7) are valid at or below the saturation density ρ_0. Efforts to constrain the behavior of the symmetry energy at higher densities are presently being pursued through observables such as π^-/π^+ ratio, K^+/K^0 ratio, neutron-proton differential transverse flow, and nucleon elliptic flow [26].

III. THE ROLE OF ISOVECTOR MESONS

A. Review of the theoretical approach

As stated in the Introduction, the starting point of our many-body calculation is a realistic neucleon-nucleon (NN) interaction, which is then applied in the nuclear medium without any additional free parameters. Thus the first question to be confronted concerns the choice of the "best" NN interaction. After the development of QCD and the understanding of its symmetries, chiral effective theories [27,28] were developed as a way to respect the symmetries of QCD while keeping the degrees of freedom (nucleons and pions) typical of low-energy nuclear physics. However, chiral perturbation theory (ChPT) has definite limitations as far as the range of allowed momenta is concerned. For the purpose of applications in dense matter, where higher and higher momenta become involved with increasing Fermi momentum, NN potentials based on ChPT are unsuitable.

Relativistic meson theory is an appropriate framework to deal with the high momenta encountered in dense matter. In particular, the one-boson-exchange (OBE) model has proven very successful in describing NN data in free space and has a good theoretical foundation. Among the many available OBE potentials, with some being part of the "high-precision generation" [29,30], we seek a momentum-space potential developed within a relativistic scattering equation, such as the one obtained through the Thompson [31] three-dimensional reduction of the Bethe-Salpeter equation [32]. Furthermore, we require a potential that uses the pseudovector coupling for the interaction of nucleons with pseudoscalar mesons. With these constraints in mind, as well as the requirement of a good description of the NN data, Bonn B [33] is a reasonable choice. The mesons included are the pseudoscalar π and η, the scalar σ and δ, and the vector ρ and ω.

As our many-body framework, we choose the Dirac-Brueckner-Hartree-Fock approach. We will now review the main aspects of our approach and the various approximations we perform through the application of the DBHF procedure.

The main strength of the DBHF approach is its inherent ability to account for important three-body forces (TBFs) through its density dependence. These are the TBFs originating from virtual excitation of a nucleon-antinucleon pair, known as "Z diagram." The characteristic feature of the DBHF method turns out to be closely related to the TBFs of the Z-diagram type, as we will argue next. In the DBHF approach, one describes the positive-energy solutions of the Dirac equation in the medium as

$$u^*(p,\lambda) = \left(\frac{E_p^* + m^*}{2m^*}\right)^{1/2}\begin{pmatrix} \mathbf{1} \\ \frac{\sigma\cdot\vec{p}}{E_p^*+m^*}\end{pmatrix}\chi_\lambda, \tag{8}$$

where the nucleon effective mass m^* is defined as $m^* = m + U_S$, with U_S being an attractive scalar potential. (This will be derived below.) It can be shown that both the description of a single-nucleon via Eq. (8) and the evaluation of the Z

diagram generate a repulsive effect on the energy per particle in symmetric nuclear matter, which depends on the density approximately as

$$\Delta E \propto \left(\frac{\rho}{\rho_0}\right)^{8/3} \tag{9}$$

and provides the saturating mechanism missing from conventional Brueckner calculations [34]. (Alternatively, explicit TBFs are used along with the BHF method in order to achieve a similar result.)

The approximate equivalence of the effective-mass description of Dirac states and the contribution from the Z diagram has a simple intuitive explanation in the observation that Eq. (8), like any other solution of the Dirac equation, can be written as a superposition of positive- and negative-energy solutions. On the other hand, the "nucleon" in the middle of the Z diagram is precisely a superposition of positive- and negative-energy states. In summary, the DBHF method effectively takes into account a particular class of TBF, which is crucial for nuclear-matter saturation.

Having first summarized the main DBHF philosophy, we now proceed to describe the DBHF calculation of IANM [11]. In the end, this will take us back to the crucial point of the DBHF approximation, Eq. (8).

We start from the Thompson [31] relativistic three-dimensional reduction of the Bethe-Salpeter equation [32]. The Thompson equation is applied to nuclear matter in strict analogy to free-space scattering and reads, in the nuclear-matter rest frame,

$$g_{ij}(\vec{q}', \vec{q}, \vec{P}, (\epsilon^*_{ij})_0) = v^*_{ij}(\vec{q}', \vec{q}) + \int \frac{d^3K}{(2\pi)^3} v^*_{ij}(\vec{q}', \vec{K}) \frac{m^*_i m^*_j}{E^*_i E^*_j} \times \frac{Q_{ij}(\vec{K}, \vec{P})}{(\epsilon^*_{ij})_0 - \epsilon^*_{ij}(\vec{P}, \vec{K})} g_{ij}(\vec{K}, \vec{q}, \vec{P}, (\epsilon^*_{ij})_0), \tag{10}$$

where g_{ij} is the in-medium reaction matrix ($ij = nn$, pp, or np), and the asterisk signifies that medium effects are applied to those quantities. Thus the NN potential v^*_{ij} is constructed in terms of effective Dirac states (in-medium spinors) as explained above. In Eq. (10), $\vec{q}$, $\vec{q}'$, and $\vec{K}$ are the initial, final, and intermediate relative momenta, respectively, and $E^*_i = \sqrt{(m^*_i)^2 + K^2}$. The momenta of the two interacting particles in the nuclear-matter rest frame have been expressed in terms of their relative momentum and the center-of-mass momentum $\vec{P}$ through

$$\vec{P} = \vec{k}_1 + \vec{k}_2 \tag{11}$$

and

$$\vec{K} = \frac{\vec{k}_1 - \vec{k}_2}{2}. \tag{12}$$

The energy of the two-particle system is

$$\epsilon^*_{ij}(\vec{P}, \vec{K}) = e^*_i(\vec{P}, \vec{K}) + e^*_j(\vec{P}, \vec{K}), \tag{13}$$

and $(\epsilon^*_{ij})_0$ is the starting energy. The single-particle energy e^*_i includes kinetic-energy and potential-energy contributions [see Eq. (27) below]. The Pauli operator Q_{ij} prevents scattering to occupied nn, pp, or np states. To eliminate the angular dependence from the kernel of Eq. (10), it is customary to replace the exact Pauli operator with its angle average. Detailed expressions for the Pauli operator and the average center-of-mass momentum in the case of two different Fermi seas can be found in Ref. [11].

With the definitions

$$G_{ij} = \frac{m^*_i}{E^*_i(\vec{q}')} g_{ij} \frac{m^*_j}{E^*_j(\vec{q})} \tag{14}$$

and

$$V^*_{ij} = \frac{m^*_i}{E^*_i(\vec{q}')} v^*_{ij} \frac{m^*_j}{E^*_j(\vec{q})}, \tag{15}$$

one can rewrite Eq. (10) as

$$G_{ij}(\vec{q}', \vec{q}, \vec{P}, (\epsilon^*_{ij})_0) = V^*_{ij}(\vec{q}', \vec{q}) + \int \frac{d^3K}{(2\pi)^3} V^*_{ij}(\vec{q}', \vec{K}) \times \frac{Q_{ij}(\vec{K}, \vec{P})}{(\epsilon^*_{ij})_0 - \epsilon^*_{ij}(\vec{P}, \vec{K})} G_{ij}(\vec{K}, \vec{q}, \vec{P}, (\epsilon^*_{ij})_0), \tag{16}$$

which is formally identical to its nonrelativistic counterpart.

The goal is to determine self-consistently the nuclear-matter single-particle potential, which, in IANM, will be different for neutrons and protons. To facilitate the description of the procedure, we will use a schematic notation for the neutron-proton potential. We write, for neutrons,

$$U_n = U_{np} + U_{nn} \tag{17}$$

and, for protons,

$$U_p = U_{pn} + U_{pp}, \tag{18}$$

where each of the four pieces on the right-hand side of Eqs. (17) and (18) signifies an integral of the appropriate G-matrix elements (nn, pp, or np) obtained from Eq. (16). Clearly, the two equations above are coupled through the np component, and so they must be solved simultaneously. Furthermore, the G-matrix equation and Eqs. (17) and (18) are coupled through the single-particle energy (which includes the single-particle potential, itself defined in terms of the G matrix). So we have a coupled system to be solved self-consistently.

Before proceeding with the self-consistency, one needs an *ansatz* for the single-particle potential. The latter is suggested by the most general structure of the nucleon self-energy operator consistent with all symmetry requirements. That is,

$$\mathcal{U}_i(\vec{p}) = U_{S,i}(p) + \gamma_0 U^0_{V,i}(p) - \vec{\gamma} \cdot \vec{p} U_{V,i}(p), \tag{19}$$

where $U_{S,i}$ and $U_{V,i}$ are an attractive scalar field and a repulsive vector field, respectively, with $U^0_{V,i}$ being the timelike component of the vector field. These fields are, in general, density and momentum dependent. We take

$$\mathcal{U}_i(\vec{p}) \approx U_{S,i}(p) + \gamma_0 U^0_{V,i}(p), \tag{20}$$

which amounts to assuming that the spacelike component of the vector field is much smaller than both $U_{S,i}$ and $U^0_{V,i}$. Furthermore, neglecting the momentum dependence of the scalar and vector fields and inserting Eq. (20) in the Dirac

equation for neutrons and protons propagating in nuclear matter,

$$[\gamma_\mu p^\mu - m_i - \mathcal{U}_i(\vec{p})]u_i(\vec{p},\lambda) = 0, \tag{21}$$

naturally lead to rewriting the Dirac equation in the form

$$[\gamma_\mu (p^\mu)^* - m_i^*]u_i(\vec{p},\lambda) = 0, \tag{22}$$

with positive-energy solutions as in Eq. (8), $m_i^* = m + U_{S,i}$, and

$$(p^0)^* = p^0 - U^0_{V,i}(p)\,. \tag{23}$$

The subscript i signifies that these parameters are different for protons and neutrons.

As in the symmetric-matter case [35], evaluating the expectation value of Eq. (20) leads to a parametrization of the single-particle potential for protons and neutrons [Eqs. (17) and (18)] in terms of the constants $U_{S,i}$ and $U^0_{V,i}$, which is given by

$$U_i(p) = \frac{m_i^*}{E_i^*}\langle\vec{p}|\mathcal{U}_i(\vec{p})|\vec{p}\rangle = \frac{m_i^*}{E_i^*}U_{S,i} + U^0_{V,i}. \tag{24}$$

Also,

$$U_i(p) = \sum_{j=n,p}\sum_{p'\leqslant k_F^j} G_{ij}(\vec{p},\vec{p}\,'), \tag{25}$$

which, along with Eq. (24), allows the self-consistent determination of the single-particle potential as explained below.

The kinetic contribution to the single-particle energy is

$$T_i(p) = \frac{m_i^*}{E_i^*}\langle\vec{p}|\vec{\gamma}\cdot\vec{p} + m|\vec{p}\rangle = \frac{m_i m_i^* + \vec{p}^{\,2}}{E_i^*}, \tag{26}$$

and the single-particle energy is

$$e_i^*(p) = T_i(p) + U_i(p) = E_i^* + U^0_{V,i}. \tag{27}$$

The constants m_i^* and

$$U_{0,i} = U_{S,i} + U^0_{V,i} \tag{28}$$

are convenient to work with as they facilitate the connection with the usual nonrelativistic framework [36].

Starting from some initial values of m_i^* and $U_{0,i}$, the G-matrix equation is solved and a first approximation for $U_i(p)$ is obtained by integrating the G matrix over the appropriate Fermi sea; see Eq. (25). This solution is again parametrized in terms of a new set of constants, determined by fitting the parametrized U_i, Eq. (24), to its values calculated at two momenta, a procedure known as the "reference-spectrum approximation." The iterative procedure is repeated until satisfactory convergence is reached.

Finally, the energy per neutron or proton in nuclear matter is calculated from the average values of the kinetic and potential energies as

$$\bar{e}_i = \frac{1}{A}\langle T_i\rangle + \frac{1}{2A}\langle U_i\rangle - m. \tag{29}$$

The EOS, or energy per nucleon as a function of density, is then written as

$$\bar{e}(\rho_n,\rho_p) = \frac{\rho_n\bar{e}_n + \rho_p\bar{e}_p}{\rho} \tag{30}$$

or

$$\bar{e}(k_F,\alpha) = \frac{(1+\alpha)\bar{e}_n + (1-\alpha)\bar{e}_p}{2}\,. \tag{31}$$

Clearly, symmetric nuclear matter is obtained as a by-product of the calculation described above by setting $\alpha = 0$, whereas $\alpha = 1$ corresponds to pure neutron matter.

B. Results

In Table I we show the contributions of some major partial waves to the potential energy of neutron matter (NM) and of symmetric nuclear matter (SNM). The last column displays their difference to signify the potential-energy contribution to the symmetry energy. The chosen density is 0.185 fm^{-3}, corresponding to a Fermi momentum of 1.4 fm^{-1} in SNM and 1.76 fm^{-1} in NM [from Eq. (3) with $\alpha = 1$]. (Summing up all contributions and including the kinetic term yields 33.7 MeV, which is very close to the actual value of our symmetry energy at this density.)

We observe that spin-triplet waves, particularly $^3S_1$, give the largest contribution. It will be interesting to revisit this point in conjunction with the role of the δ meson. We note that, although the contribution of the δ meson to a quantitative NN interaction is known to be relatively small, this meson is a crucial mechanism to fine-tune the S waves, that is, $^1S_0$ vs $^3S_1$. Hence, its importance for isospin-dependent phenomena.

In Table II, we show the contributions to the potential energy of SNM from the different mesons. We show these contributions for potentials A and C as well [33]. The three potentials differ mostly in the parameters used for the πNN form factor, which has a large impact on the strength of the tensor force, with Bonn A displaying the weakest tensor force and Bonn C the strongest (as demonstrated by the predicted D-state probabilities, which are 4.47%, 5.10%, and 5.53% for A, B, and C, respectively.) These three potentials span the uncertainty in our knowledge of the short-range tensor force. Considering all three models will then provide information on how the effects being examined (namely, the role of the isovector mesons on the symmetry energy) change with changing tensor force while maintaining consistency with the

TABLE I. Potential energy contributions (in MeV) for selected partial waves to the energy of NM and SNM and their difference. The density is equal to 0.185 fm^{-3}.

Partial waves	$U_{\rm NM}$	$U_{\rm SNM}$	$U_{\rm NM} - U_{\rm SNM}$
$^1S_0$	−18.71	−18.75	0.042
$^3P_0$	−1.88	−1.75	−0.126
$^1P_1$	0	4.045	−4.045
$^3P_1$	20.51	14.40	6.111
$^3S_1$	0	−20.29	20.29
$^3D_1$	0	1.564	−1.564
$^1D_2$	−4.250	−2.477	−1.773
$^3D_2$	0	−4.360	4.360
$^3F_2$	−1.022	−0.560	−0.462
$^3P_2$	−12.47	−7.697	−4.773

TABLE II. Contributions (in MeV) to the potential energy of SNM from various mesons for three different potential models. The density is equal to 0.185 fm^{-3}.

Potential	$\sigma+\omega$	$\sigma+\omega+\pi$	π	$\sigma+\omega+\pi+\rho$	ρ	$\sigma+\omega+\rho+\delta$	δ	All mesons
Bonn B	−29.82	−45.89	−17.08	−38.69	7.21	−35.13	3.56	−34.24
Bonn A	−33.27	−44.65	−11.38	−38.47	6.18	−36.90	1.57	−36.15
Bonn C	−23.45	−45.21	−21.75	−38.74	6.47	−33.61	5.13	−32.98

free-space NN data. We believe that the latter constraint is crucial for a reliable investigation of many-body effects.

We start by taking σ and ω together since a model with only one of these mesons is entirely meaningless and would produce a completely unrealistic correlated wave function, especially so with σ alone, due to the absence of any short-range repulsion. The fourth column is the difference between the values shown in the third and second columns and represents the contribution from the pion alone. Notice that this contribution is attractive, as to be expected, recalling that the pion's tensor potential V_t generates a large and attractive second-order term $V_t \frac{Q}{E_0-E} V_t$ when iterated in the Bethe-Goldstone equation. Consistent with that, this contribution is largest with Bonn C due to its stronger tensor force.

The contribution of the ρ meson is shown in the sixth column as the difference between the values in columns five and three. It is considerably smaller than the pion's and is repulsive since the tensor force generated by ρ typically reduces the pion's tensor force at short range. With regard to ρ, it is useful to recall that the interaction Lagrangian that couples vector mesons with nucleons contains both a vector coupling and a tensor coupling,

$$\mathcal{L}_{NN\rho} = -g_\rho \bar{\psi}\gamma_\mu \vec{\tau}\psi \cdot \phi_\rho^\mu - \frac{f_\rho}{4M}\bar{\psi}\sigma_{\mu\nu}\vec{\tau}\psi \cdot \left(\partial^\mu \phi_\rho^\nu - \partial^\nu \phi_\rho^\mu\right). \tag{32}$$

These are related to the electromagnetic properties of the nucleon in the vector dominance model, where the nucleon couples to the photon *via* a vector meson. In the framework of the vector dominance model [37], a value of 3.7 is obtained for the ratio of the tensor-to-vector coupling constant, $\kappa_\rho = f_\rho/g_\rho$, whereas a stronger value of $\kappa_\rho = 6.6$ was determined from partial-wave analyses [38]. In other words, a larger value of the ρ tensor coupling as compared to its vector coupling is well supported by evidence, a fact that is reflected in meson-exchange models where, typically, the ratio κ_ρ is about 6. Therefore, a Lagrangian density with only a vector coupling for ρ [39], i.e., $f_\rho = 0$, may miss the most important part of how this meson couples to the nucleon.

In Table II, the δ meson is included next, providing a small and positive contribution. The last column displays the full result, when the pseudoscalar meson η is included as well. Table II is more insightful when examined together with Table III. The latter shows the same physical quantities as in Table II but for pure neutron matter. Here the contribution of the pion is much smaller and opposite in sign. This is due to the absence of the $^3S_1$ partial wave in NM and, consequently, the absence of a large part of the attractive second-order tensor term mentioned above. The effect of the δ meson in NM is of about the same size as the one observed in SNM but opposite in sign. This can be easily understood recalling that the effect of the isovector scalar meson is attractive in $^1S_0$ and repulsive in $^3S_1$ and that the latter is absent from NM. With respect to potential model dependence, the size of the effect is largest in model C and weakest in model A. Model dependence should be expected, as the parameters of the δ meson are quite different for the three potentials.

Before proceeding to discuss the symmetry energy, we show, for Bonn B, how the various mesons contribute to the energy of symmetric nuclear matter [Fig. 1(a)] and neutron matter [Fig. 1(b)]. From Fig. 1(a), one can see that the effect of the pion is large at all densities. As argued previously, this effect comes from the attractive second-order contribution generated by the pion potential, which is clearly quite large already at low density. As density increases, the second-order tensor contribution is reduced by the Pauli operator (and dispersion effects) and thus retains approximately the same size. We also note the clear impact of the pion on the saturation density of SNM, demonstrating the remarkable saturating effect generated by the tensor force, particularly through the $^3S_1$ partial wave.

For neutron matter, on the other hand, the contribution of the pion comes mostly from the (repulsive) tensor force in some major isospin-1 partial waves. Accordingly, Fig. 1(b) shows that such a contribution is opposite in sign and weaker as compared to the one in SNM, as already observed when discussing Table III. Also, the effect increases with density, in contrast to the case of SNM; see comments in the previous paragraph.

TABLE III. As in Table II but for NM.

Potential	$\sigma+\omega$	$\sigma+\omega+\pi$	π	$\sigma+\omega+\pi+\rho$	ρ	$\sigma+\omega+\rho+\delta$	δ	All mesons
Bonn B	−17.00	−13.30	3.7008	−12.00	1.30	−15.21	−3.22	−16.09
Bonn A	−20.10	−15.50	4.60	−14.00	1.50	−15.23	−1.23	−16.40
Bonn C	−14.04	−11.37	2.67	−10.39	0.98	−15.48	−5.11	−16.05

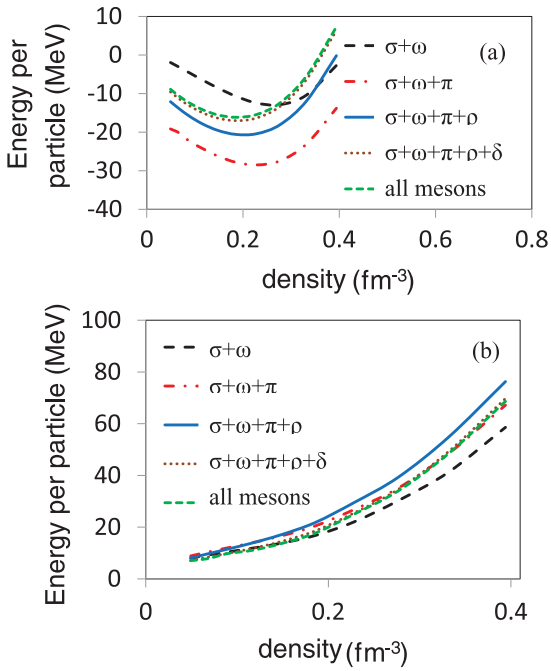

FIG. 1. (Color online) Contribution from the various mesons to the equation of state of (a) symmetric matter and (b) neutron matter.

In Table IV, we show the difference between the potential energy contributions to NM and SNM from the isovector mesons as an estimate of the effect of each meson on the potential-energy part of the symmetry energy. (The density is the same as in the previous tables.) Clearly, in a microscopic, meson-theoretic approach the impact of the pion on the symmetry energy is the largest. We find this to be a point of considerable interest since mean-field theories are generally pionless. This is because the bulk of the attraction-repulsion balance needed for a realistic description of nuclear matter can be technically obtained from σ and ω only, an observation that is at the very foundation of Walecka models such as QHD-I [16]. However, in any fundamental theory of nuclear forces, the pion is the most important ingredient. Chiral symmetry is spontaneously broken in low-energy QCD, and the pion emerges as the Goldstone boson of this symmetry breaking [28]. Moreover, NN scattering data cannot be described without the pion, which is also absolutely crucial for the two-nucleon bound state, the deuteron.

When moving to nuclear matter (and regardless of the possibility of obtaining realistic values of its bulk properties, including the symmetry energy, with a pionless theory), this conceptual problem is not removed. Isospin dependence is carried by the isovector mesons: Because of their isovector nature, these mesons contribute differently in different partial waves, thus giving rise to isospin dependence. (This is not the case with isoscalar mesons, which tend to contribute similarly in all partial waves.) Thus, an important aspect of the physics is missing in a discussion of isospin dependence that does not include the pion. Also, conclusions concerning the effect of other mesons (particularly ρ and δ) may be distorted due to the absence of the pion. This may include, for instance, observations concerning isospin-sensitive quantities, such as the neutron-proton mass splitting in neutron-rich matter.

TABLE IV. The difference between the potential energy contributions (in MeV) to NM and SNM from isovector mesons.

Potential	$U^{\pi}_{\rm NM} - U^{\pi}_{\rm SNM}$	$U^{\rho}_{\rm NM} - U^{\rho}_{\rm SNM}$	$U^{\delta}_{\rm NM} - U^{\delta}_{\rm SNM}$
Bonn B	20.78	−5.90	−6.78
Bonn A	15.98	−4.68	−2.80
Bonn C	24.42	−5.48	−10.24

As mentioned earlier, investigations of ρ and δ contributions to the potential symmetry energy have been reported, such as the one in Refs. [14,40]. In Fig. 6-1 of Ref. [14], for instance, those contributions are shown to be very large in size (about −40 and 50 MeV at saturation density for δ and ρ, respectively). Thus, the interplay between ρ and δ is described as the equivalent, in the isovector channel, of the σ-ω interplay in the isoscalar channel [40].

The dramatic differences between those and our present observations originate from several sources, which include the absence of the pion, the nature of the ρ coupling, and the fact that our meson contributions, when iterated, are reduced by the effect of the Pauli projector. As mentioned previously, the role of the δ is important although subtle, and it is found in its different contributions to $I = 1$ and $I = 0$ partial waves, especially the S waves.

In Fig. 2 we show the density dependence of the symmetry energy with Bonn A, B, and C. The potential model dependence comes almost entirely from differences among predictions of the SNM energy. With the three sets of predictions, we mean to estimate the uncertainty to be expected when using different parametrizations for the isovector mesons while respecting the free-space NN data.

Figure 3 displays the momentum dependence of the single-proton and single-nucleon potentials in IANM, as predicted by the three potentials. Differences are small, at most 10% at the lowest momenta. We recall that the gradient between the potentials shown in Fig. 2, closely related to the isovector optical potential, is the crucial mechanism that separates proton and neutron dynamics in IANM.

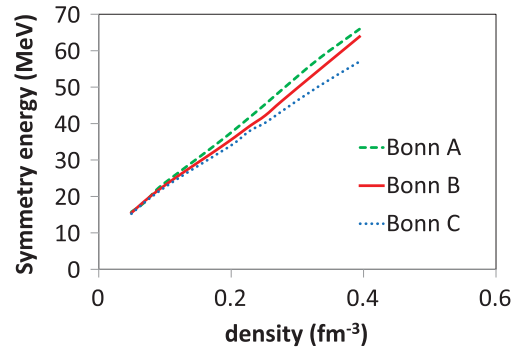

FIG. 2. (Color online) The symmetry energy as predicted with Bonn A, B, and C.

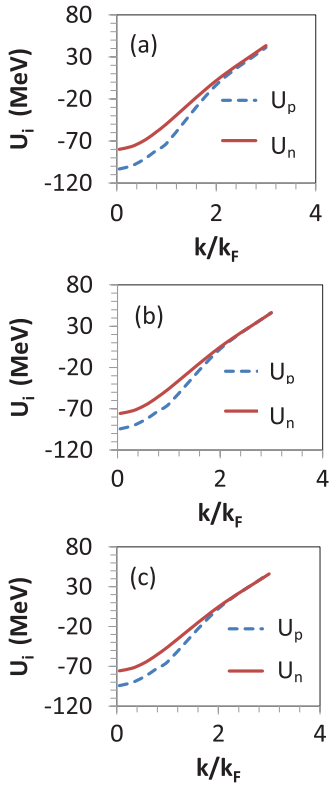

FIG. 3. (Color online) Momentum dependence of the single-nucleon potentials in IANM U_i $(i = p, n)$ predicted with Bonn (a) A, (b) B, and (c) C. The total density is equal to 0.185 fm^{-3}, and the isospin asymmetry parameter is 0.4. The momentum is given in units of the Fermi momentum, which is equal to 1.4 fm^{-1}.

In concluding this section, we take note of Ref. [41], where the effect of the short-range tensor interaction on the symmetry energy is examined using an approximate expression for the second-order tensor contribution [42]. It must be noted, however, that the variations performed on the short-range tensor interaction in Ref. [41] are unconstrained and thus to some extent arbitrary.

IV. CONCLUSIONS

We have examined the effect of the isovector mesons on the difference between the potential energies of pure neutron matter and symmetric matter. Our findings are easily understood in terms of the contributions of each meson to the appropriate component of the nuclear force and the isospin dependence naturally generated by isovector mesons.

We find that the pion gives the largest contribution to this difference. The contribution of the pion is often overlooked, possibly because this meson is missing from some mean-field models, which are popular among users of equations of state. It is our opinion that conclusions regarding the interplay of ρ and δ in phenomenological models must be taken with caution.

We comment on fundamental differences between our approach and the one of mean-field models, particularly pionless QHD theories. First, these differences are of conceptual relevance since free-space NN scattering and the bound state are, essentially, pion physics. Furthermore, they can impact in a considerable way conclusions with regard to isospin-dependent systems and phenomena. In order to have a fundamental basis, a microscopic theory of the nuclear many-body problem has to start from the bare NN interaction with all its ingredients.

ACKNOWLEDGMENT

Support from the US Department of Energy under Grant No. DE-FG02-03ER41270 is acknowledged.

[1] K. A. Brueckner, S. A. Coon, and J. Dabrowski, Phys. Rev. **168**, 1184 (1968).
[2] P. J. Siemens, Nucl. Phys. A **141**, 225 (1970).
[3] M. Beiner, H. Flocard, N. V. Giai, and P. Quentin, Nucl. Phys. A **238**, 29 (1975).
[4] Y. Sugahara and H. Toki, Nucl. Phys. A **579**, 557 (1994).
[5] J. R. Stone and P.-G. Reinhard, Prog. Part. Nucl. Phys. **58**, 587 (2007).
[6] I. E. Lagaris and V. R. Pandharipande, Nucl. Phys. A **359**, 349 (1981).
[7] A. Akmal, V. R. Pandharipande, and D. G. Ravenhall, Phys. Rev. C **58**, 1804 (1998).
[8] I. Bombaci and U. Lombardo, Phys. Rev. C **44**, 1892 (1991).
[9] W. Zuo, I. Bombaci, and U. Lombardo, Phys. Rev. C **60**, 024605 (1999).
[10] L. Engvik, M. Hjorth-Jensen, E. Osnes, G. Bao, and E. Ostgaard, Phys. Rev. Lett. **73**, 2650 (1994); L. Engvik, E. Osnes, M. Hjorth-Jensen, G. Bao, and E. Østgaard, Astrophys. J. **469**, 794 (1996).
[11] D. Alonso and F. Sammarruca, Phys. Rev. C **67**, 054301 (2003).
[12] F. Sammarruca, Int. J. Mod. Phys. E **19**, 1259 (2010).
[13] E. N. E. van Dalen, C. Fuchs, and A. Faessler, Nucl. Phys. A **74**, 227 (2004).
[14] V. Baran, M. Colonna, V. Greco, and M. Di Toro, Phys. Rep. **410**, 335 (2005).
[15] J. Rizzo *et al.*, Nucl. Phys. A **732**, 202 (2004).
[16] J. D. Walecka, Ann. Phys. (NY) **83**, 491 (1974).
[17] B. D. Serot and J. D. Walecka, Adv. Nucl. Phys. **16**, 1 (1986).
[18] B. D. Serot and J. D. Walecka, Int. J. Mod. Phys. E **6**, 515 (1997).
[19] A. W. Steiner, Phys. Rev. C **74**, 045808 (2006), and references therein.
[20] W. Trautmann *et al.*, arXiv:0907.2822 [nucl-ex]; C. Sfienti *et al.*, Phys. Rev. Lett. **102**, 152701 (2009).
[21] M. B. Tsang, Y. Zhang, P. Danielewicz, M. Famiano, Z. Li, W. G. Lynch, and A. W. Steiner, Phys. Rev. Lett. **102**, 122701 (2009).
[22] V. Greco, Int. J. Phys. E **19**, 1664 (2010).
[23] B. Borderie and M. F. Rivet, Prog. Part. Nucl. Phys. **61**, 551 (2008); arXiv:0812.3524 [nucl-ex].
[24] G.-C. Yong, Int. J. Phys. E **19**, 1647 (2010).
[25] Z.-Q. Feng, Int. J. Phys. E **19**, 1686 (2010).
[26] C. M. Ko, Int. J. Phys. E **19**, 1763 (2010).

[27] S. Weinberg, Phys. Lett. B **251**, 288 (1990).
[28] R. Machleidt and D. R. Entem, Phys. Rep. **503**, 1 (2011).
[29] R. Machleidt, Phys. Rev. C **63**, 024001 (2001).
[30] V. G. J. Stoks, R. A. M. Klomp, C. P. F. Terheggen, and J. J. de Swart, Phys. Rev. C **49**, 2950 (1994).
[31] R. H. Thompson, Phys. Rev. D **1**, 110 (1970).
[32] E. E. Salpeter and H. A. Bethe, Phys. Rev. **84**, 1232 (1951).
[33] R. Machleidt, Adv. Nucl. Phys. **19**, 189 (1989).
[34] G. E. Brown *et al.*, Comments Nucl. Part. Phys. **17**, 39 (1987).
[35] R. Brockmann and R. Machleidt, Phys. Lett. B **149**, 283 (1984).
[36] M. I. Haftel and F. Tabakin, Nucl. Phys. A **158**, 1 (1970).
[37] J. J. Sakurai, *Currents and Mesons* (University of Chicago Press, Chicago, 1969).
[38] G. Höhler and E. Pietarinen, Nucl. Phys. B **95**, 210 (1975).
[39] J. Boguta and C. E. Price, Nucl. Phys. A **505**, 123 (1989).
[40] B. Liu, V. Greco, V. Baran, M. Colonna, and M. Di Toro, Phys. Rev. C **65**, 045201 (2002).
[41] A. Li and B.-A. Li, arXiv:1107.0496 [nucl-th].
[42] G. E. Brown and R. Machleidt, Phys. Rev. C **50**, 1731 (1994).